International Core Journal of Engineering Volume 6 Issue 12, 2020
ISSN: 2414-1895 DOI: 10.6919/ICJE.202012_6(12).0041

Visual Servo-based Method for Bridge Crossing of Unmanned Surface Vehicle

Junxia Zhao[1,a], Jianhua Wang[1,b] and Xiang Zheng[1,c]

[1]Shanghai Maritime University, Shanghai 203106, China.

[a]1186242427@qq.com, [b]jian-hua.wang@163.com, [c]xiangzheng@shmtu.edu.cn

Abstract

With the increasing applications of Unmanned Surface Vehicles (USV), the complexity of navigable waters is also increasing. This paper proposes a navigation method using visual servo to accommodate outlier and loss of GPS signals near and under bridges so as to enhance the ability of USV to sail through the bridge safely. Firstly, the real-time scene of the bridge is collected through the visual system carried by the USV when preparing to sail through the bridge. Then the region of bridge aperture in the image is segmented by image preprocessing and threshold segmentation . With the extracted contour of the segmented region of the bridge aperture, the heading deviation angle and deviation distance are calculated and feed to the controller which adjusts the heading and speed of the USV in real time to drive the USV through the bridge safely. Finally, the performance of the proposed method is verified with real pictures taken by USV in actual environment. Simulation and experiment results show that the proposed algorithm achieves 96% accuracy rate for bridge aperture detection, and 100% safe driving rate when the starting point is within a distance of 4m from the center line of the bridge, which basically meets the requirements for safe sailing of the USV through the bridge.

Keywords

Unmanned surface vehicle; Sail through the bridge; Visual servo.

1. Introduction

In recent years, USV industry has developed rapidly benefitting from the continuous advancement of artificial intelligence and other technologies, and USVs have been widely used in military and civilian fields. China Classification Society clearly defines that smart ships need to have perception capabilities, memory and thinking capabilities, learning and adaptive capabilities, and behavioral decision-making capabilities [1]. At present, the mainstream USV realizes the needs of smart ships by carrying a fusion sensor system combining inertial navigation system (INS) and global positioning system (GPS). However, when USV is sailing near and under bridges or there are large waterside constructions, GPS signals are restricted or unavailable due to unknown disturbance. In the " Mission at Sea", a competition of China USV Challenge, sponsored by Chinese Society of Naval Architecture and Marine Engineering, Project B requires the participants to cross Wanpingkou Bridge in the shape of an "8" [2]. Due to abnormal GPS signals caused by the wide bridge deck and the surrounding electromagnetic interference, many groups' USV collided with the bridge piers. Data analysis shows abnormal values of HDOP (horizontal dilution of precision) when crossing the Wanpingkou Bridge, which is used to measure the accuracy of GPS, see Figure 1.

Aiming at low-connected navigation of USV under the limitation of GPS, Ko N Y[3][4] expanded the Kalman filter to fuse multi-sensor data to eliminate abnormal GPS values and estimate the true positioning of the hull, and pointed out that the more fusion measurement data, the more accurate

ISSN: 2414-1895 DOI: 10.6919/ICJE.202012_6(12).0041

navigation would be. Experts and scholars at home and abroad also use other sensors to make up for the shortage of GPS and enhance the environment perception of USV. Woo J [5] adopts visual sensor to identify obstacles on water surface, and takes motion information of target and visual sensor information as the input of fuzzy controller to obtain collision risk rate. Wang H [6-7] gives a vision-based water surface obstacle detection method.Use saliency detection to obtain the potential area of the obstacle, and then adopt Harris corner detection to extract the corner feature to estimate the motion of the potential obstacle to judge whether it is true. Experiments show that this method can be applied to a speed of 12 knots USV for real-time detection of obstacles within 30-100m. Almeida C [8], uses ship-borne radar for obstacle detection, but it is difficult to detect small obstacles located within 200m of the ship. Meanwhile, power consumption and volume of radar are also challenges for small USV.J. Muhovič [9] uses fast semantic segmentation to figure out the horizontal direction, and combines three-dimensional visual point cloud data to obtain the obstacle position information ,which can reduce the false alarm phenomenon.Autonomous bridge crossing for USV can also be classified as a problem of autonomous obstacle avoidance, but to date, the problem has received scant attention. Han J [10-11] identifies bridge structures (such as bridge piers) by fusing camera images and point cloud data provided by lidar sensors, and combines all position-related information from INS, Doppler Velocimeter (DVL), and geometric information of the detected bridge to reconstruct the scene under the bridge tunnel in three dimensions.Huang[12],uses binocular direct sparse mileage calculation method to construct a three-dimensional space model of water environment with bridges, converts the constructed three-dimensional point cloud image into a two-dimensional grid image and marks obstacles. However, obstacle avoidance system is not designed.

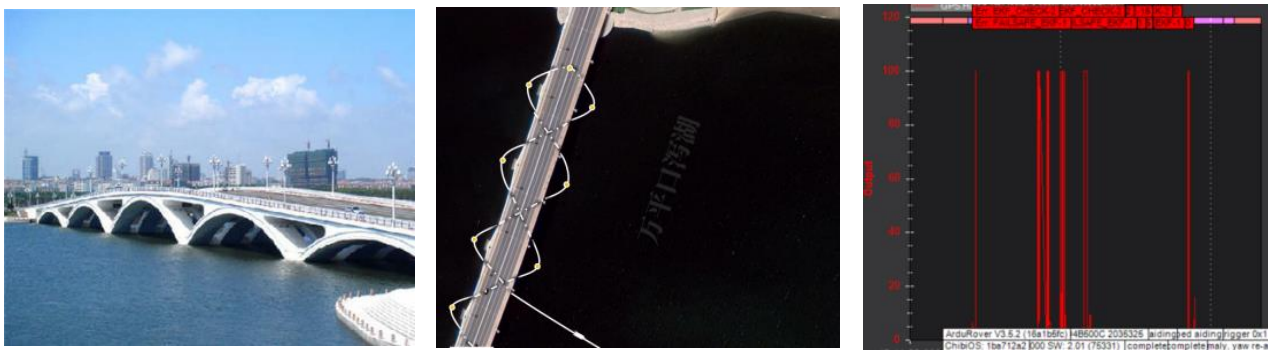

(a) (b) (c)

Figure 1 (a)Wanpingkou Bridge (b)"Mission at Sea" Class B Project Mission Path(c)Unusual HDOP anomaly

Combining the unique environmental characteristics of the bridge aperture, that is, the contrast between the dark inside and the external light is large and integral, this paper proposes a navigation method based on visual servo to improve the ability of USV to safely pass the bridge.

2. System Description

This article takes USV "Haixiang" as the research object, which is developed by Marine Technology & Control Engineering Key Laboratory of Shanghai Maritime University, as shown in Figure 2. "Haixiang" is 1.6m long and 1.2m wide, with no bow propeller and stern thruster, no rudder. It has two brushless motors installed at the tail of the hull, and we can adjust the voltage of the propulsion motors on both sides by changing the PWM signal, so that "Haixiang" makes use of the left and right motor differential speed to change the speed and heading. Motion equation and dynamic model reference is illustrated in paper[13]. Since the propulsion equipment of the "Haixiang" can only control three degrees of freedom of the hull along the horizontal plane, this article only considers the boat's forward, yaw, and lateral drifting motions, and ignores the boat's heave, roll, and pitch motions.

ISSN: 2414-1895 DOI: 10.6919/ICJE.202012_6(12).0041

Figure 2. HaiXiang USV

3. Method of Sailing Through the Bridge with Visual Servo

3.1 Extract the Contour of Bridge Aperture

3.1.1. Image preprocessing

In this paper, the contour of the bridge aperture is the main extraction feature. It is difficult to identify and extract the contours of various forms of bridge apertures due to the influence of surrounding obstacles and water reflections. It is necessary to preprocess the pictures taken by USV. The internal dimness of the bridge aperture has a large and holistic contrast with the external brightness. Firstly, the contrast of the collected bridge aperture images is adjusted with Equation (1):

$$g(x) = af(x) + \beta \tag{1}$$

$f(x)$ is the original image, $g(x)$ is the output image, α is the gain used to set the image contrast, β is the bias used to adjust the image brightness. Figure. 3 (a) is the original picture taken by the on-board camera. Set α=2, β=50 and the result of contrast adjustment is shown in Figure. 3 (b).In this paper, the selection of controlled variables is only related to the transverse coordinates of the bridge aperture contour in the window. It can be seen that the extraction accuracy has little impact although the scope of the bridge aperture is expanded after contrast adjustment.At the same time, some unrelated features can be ignored to reduce the difficulty of detection.

(a) (b) (c)

Figure 3. Image preprocessing

3.1.2. Extract the contour

The bridge aperture is obvious after preprocessing. The brightness contrast will be reflected in the difference of gray value. After gaussian filtering, the image is binarized with 250 as the threshold, and then the contour is extracted. Many small contours will be produced due to the influence of water reflection, so only the outline with a certain area will be retained. Then the enclosing rectangle of the contour is obtained. Figure 3 (c) is the bridge aperture contour extracted from Figure 3 (a).

In this paper, the left and right sides of the rectangular frame are considered to be the left and right profiles of the bridge aperture.

ISSN: 2414-1895 DOI: 10.6919/ICJE.202012_6(12).0041

3.2 Visual Servo

Since the strategy mentioned in this paper is mainly used to make up for the failure of shipborne navigation equipment such as GPS due to the limitation of bridge, the visual servo method assumes that the camera can observe the bridge. When USV is moving, the position and course of the hull constantly change, and the image of the bridge aperture calculated by the linear imaging model shown on camera screen also changes along with it.

The following bridge profiles will appear in the camera window:

a) The left and right profile of bridge aperture.When USV is preparing to cross the bridge, both sides of the bridge aperture can be observed in most practical situations.

b) Single profile of bridge aperture.This condition occurs when the angle between heading and the bridge's vertical line is too large.

c) None. When USV moves to the end of the bridge aperture ,there will be no profiles of aperture due to the limitation of the camera field Angle. At this stage, the USV has no risk of collision, and the control strategy is to maintain the current course and continue sail straight.If the profile does not appear in the camera window for a period of time, the USV can be considered to have successfully crossed the bridge

In the first two case, the controlled variable is selected in the following section:

3.2.1 Double profiles

As shown in Figure 4, the rectangle is considered to be the camera window. According to the camera resolution, the rectangle is set to be 1280 in length and 1024 in width. The coordinate system is established with the upper left vertex of the window as the origin of coordinates, the horizontal axis as the X-axis, and the longitudinal axis as the Y-axis.

Among them, point M is in the middle line of the camera window, point P is in the middle line of the left and right outline, line C_lD_l, C_rD_r are the profiles at a certain time.Deviation distance and deviation Angle are selected as the controlled variables, and the calculation formula is as follows:

$$\begin{cases} \theta = \arctan\left(\dfrac{640-(X_P-X_M)}{f}\right) \\ L=(rdis-ldis)/k \end{cases} \tag{2}$$

Where X_p, X_M is the X-axis coordinate of P and M; f is the camera focal length; $ldis$ is the transverse distance from the left contour to the left boundary of the window; $rdis$ is the transverse distance from the right contour to the right boundary of the window; k is the proportional coefficient.

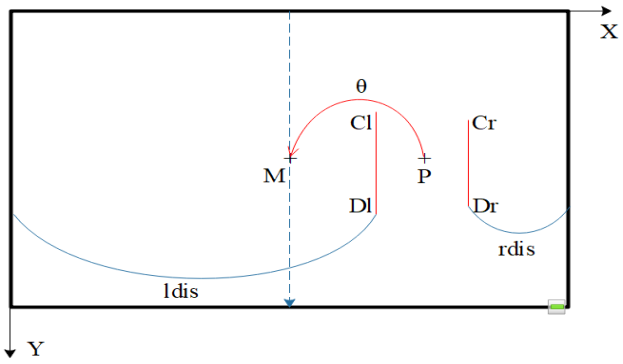

Figure 4. Control variables of bilateral profile

3.2.2 Single profile

When only one profile exists, the deviation distance is selected as the controlled variable, and the calculation formula is as follows:

ISSN: 2414-1895 DOI: 10.6919/ICJE.202012_6(12).0041

$$L=\begin{cases}-ldis/k, left\ profile\\ rdis/k, right\ profile\end{cases} \tag{3}$$

3.3 Control Method

The block diagram of the control system is shown in Figure 5. Firstly, the real-time scene of the bridge is taken and the contour lines on both sides of the bridge aperture are obtained through the image processing module. According to the different situation of the contour line extracted from the window, the mode is judged; The sum of the controlled variables, heading deviation angle and deviation distance are calculated and feed to the PD controller which controls the course of USV in real time by differential adjustment of the voltage of the propulsion motors on both sides of the vessel to make it pass through the bridge, and the calculation formula is as follows:

$$\begin{cases}\Delta u=k_p(\theta+L)+k_d w\\ U_l=U_0-\Delta u\\ U_r=U_0+\Delta u\end{cases} \tag{4}$$

Where K_p and K_d are proportional control coefficient and integral control coefficient respectively; ω is the rotational angular velocity of USV; U_0 is the reference voltage. If the profile does not appear in the camera window for a period of time, the USV can be considered to have successfully crossed the bridge. The voltage of motors on both sides will be set as reference voltage, and the USV moves forward along the course at the previous moment.

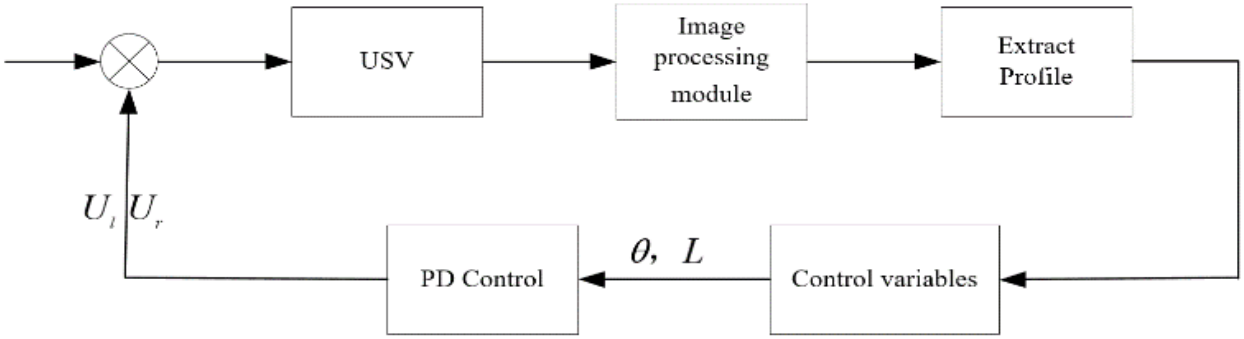

Figure 5. Control system diagram

3.4 Evaluation Index

According to diverse sizes of bridge and USV, we can set a safe distance D_{safe}. Recognize $D_l(i)$, $D_r(i)$ as the distance from USV to both sides of the bridge aperture, $Rate_{safe}$ as safety driving rate which is taken as evaluation index. The calculation formula is as follows:

$$Rate_{safe}=\min\left(\frac{Count_l}{Sum_1},\frac{Count_r}{Sum_r}\right) \tag{5}$$

Where $Count_l$, $Count_r$ is the amount of $D_l(i)>D_{safe}$, $D_r(i)>D_{safe}$, and Sum_l, Sum_r is the amount of all measurement points in this process.

4. Simulation and Experiment

4.1 Simulation

The dynamic model of "Haixiang" is adopted to verify the correctness and effectiveness of the visual servo method proposed in this paper. The pixel focal length of the camera is set at 1050 and the image resolution is 1280*1024.

ISSN: 2414-1895 DOI: 10.6919/ICJE.202012_6(12).0041

4.1.1 Single bridge aperture

The simulation environment construction of a single bridge aperture is shown in Figure 6. Two cuboids are drawn as the bridge piers in the three-dimensional coordinate system to simulate the scene of a single bridge aperture with a width of 4m and a height of 3m. The USV moves on the XOY plane. We take line C_lD_l , C_rD_r as the left and right bridge aperture contour that need to be recognized, wherein, C_l's coordinate is(-2,5,3), D_l's coordinate is(-2,5,0), C_r's coordinate is(2,5,3), D_r's coordinate is(2,5,0).

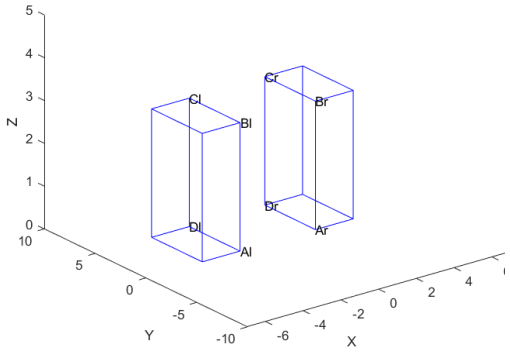

Figure 6. Single aperture in simulation

This part USV starts from different starting points to verify and compare the performance of bridge apreture crossing by visual servo. Set parameters of PD controller as K_p =10, $Kd=8$.

USV starts from(-6,-15),(-3,-15),(0,-15),(3,-15),(6,-15), and the initial heading is 90°. Different trajectories is shown in Figure 7 (a). All five groups successfully cross the bridge. Recognize the trajectories starting from point (-6,-15),(-3,-15) as track A and track B respectively.Since trajectories departing from different points have symmetry, we will focus on trajectory A and Trajectory B. Figure 7 (b) shows the curve of the controlled variables of trajectory A and B over time.At the initial moment, the starting points of A and B are all located to the left of the center line of the bridge aperture, and the contour imaging of both sides of the bridge aperture is located to the right of the window, $L<0$, $\theta<0$, Therefore, $\Delta u<0, U_l>U_r$,the USV moves to the right.As the starting point of A is far away from the bridge aperture at the initial time, according to formula (2), $L_a>L_b, \theta_a>\theta_b$, A has a stronger control effect than B in the first half process, and the motion trajectory converges faster.The USV gets closer and closer to the bridge aperture, and its images in the window show the progressive symmetry of the middle line of the window, L_a, L_b, θ_a and θ_b all tend to 0. The USV maintains the current course and passes through the bridge.

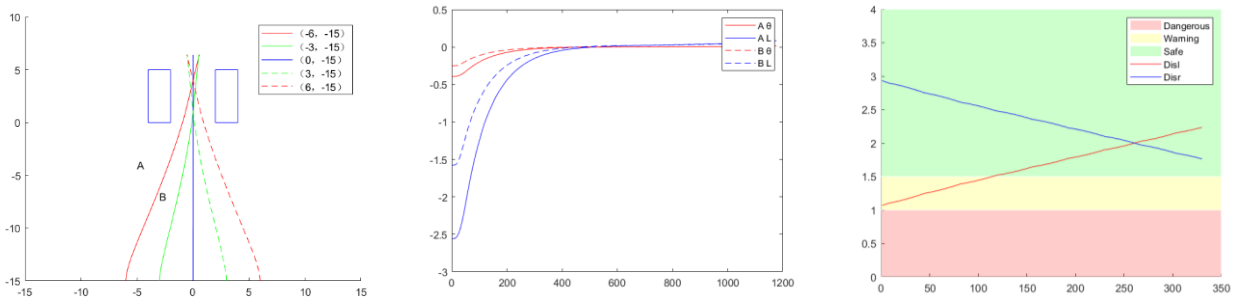

(a) (b) (c)

Figure 7 (a)Trajectories of different starting points in single aperture simulation (b)Control variables of starting at (-6,-15), (-3,-15)(c)Performance of the trajectory starting at(-6,-15)

ISSN: 2414-1895 DOI: 10.6919/ICJE.202012_6(12).0041

Fig. 7 (c) shows the distance between the center of the hull and both sides of the bridge prerture along track A.Since the bridge aperture is 4m wide and the ship is 1.2m wide,the distance between 1m and 1.5m is set as the danger zone, between 1m and 1.5m as the warning zone, and above 1.5m as the safety zone.

Table 1 shows the performance indexes of 7 groups of bridge crossing from different starting points.The starting point of track A is far away from the center line of the bridge hole, and the safe sailing rate is 65%. When entering the bridge aperture, the distance between the hull and piers is located in the warning area. However, at this time, the direction of the USV is pointing to the center line of the bridge, and no collision will occur if it continues to drive.

The simulation results show that the method using visual servo for bridge crossing can reach 100% safe driving rate within 4m of the starting point deviating from the center line of the bridgeaperture.

Table 1. Performance of Different Starting Points in Simulation of Crossing a Single Aperture

Start place	Minimum distance /m		Mean distance/m		Safe driving rate
	Disl	Disr	Disl	Disr	
(-6,-15)	1.07	1.76	1.67	2.33	65%
(-5,-15)	1.34	1.71	1.83	2.17	85%
(-4,-15)	1.61	1.67	1.98	2.02	100%
(-3,-15)	1.89	1.61	2.15	1.85	100%
(0,-15)	2.00	2.00	2.00	2.00	100%
(3,-15)	1.62	1.88	1.86	2.14	100%
(6-15)	1.77	1.06	2.34	1.66	65%

4.1.2 Double bridge aperture

Sometimes USV is also faced with continuous bridge apertures crossing.Therefore, double bridge apertures is built in the simulation environment, as shown in Figure 8. Four cuboids are drawn as the piers to simulate two bridge apertures with a width of 4m and a height of 3m. Before the second bridge, the left and right bridge aperture contour lines needed to be recognized are $dC_l dD_l$, $dC_r dD_r$, wherein, dC_l 's coordinate is (-6,25,3), dD_l 's coordinate is (-6,25,0), dC_r 's coordinate is (-2,25,3), dD_r 's coordinate is (-2,25,0).

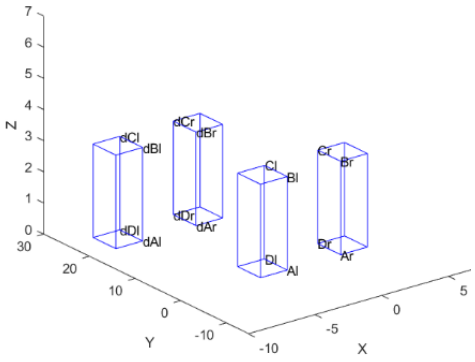

Figure 8. Double apertures in simulation

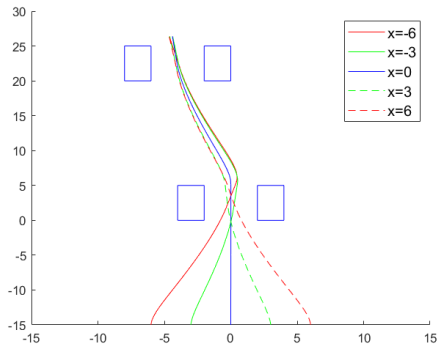

Figure 9. Trajectories of different starting points in double apertures simulation

In double bridge apertures simulation, the parameters are set the same as the simulation of single bridge aperture, and the starting points are selected as (-6,-15),(-3,-15),(0,-15),(3,-15),(6,-15). Five groups' tracks are shown in Figure 9, all of which successfully crossed the double bridge apertures.

ISSN: 2414-1895 DOI: 10.6919/ICJE.202012_6(12).0041

Table 2 shows the performance of 5 groups of double bridge apertures crossing from different starting points.Different from Table 1, the minimum distance, average distance and safe driving rate listed in the table are all counted during the whole process of crossing the double bridge apertures.

According to the data in the table 2, it can be concluded that when the starting point deviates far from the center line of the bridge aperture, the safe sailing rate of USV is slightly lower. Within a certain range of the starting point deviates from the center line of the bridge aperture, the method using visual servo for bridge crossing can achieve 100% safe sailing rate.

Table 2.

Start place	Minimum distance /m		Mean distance/m		Safe driving rate
	Disl	Disr	Disl	Disr	
(-6,-15)	1.22	1.47	1.92	2.08	89%
(-3,-15)	1.78	1.51	2.18	1.82	100%
(0,-15)	1.73	1.70	2.00	2.00	100%
(3,-15)	1.57	1.84	1.80	2.10	100%
(6,-15)	1.53	1.20	2.04	1.96	88%

4.2 Field Experienment

We choosed a square bridge aperture in the campus of Shanghai Maritime University for image acquisition to test the performance of the contour detection algorithm mentioned in this paper, as shown in Figure 10.

Figure 10. Scene of bridge crossing

Since the strategy mentioned in this paper is mainly used to make up for the failure of shipborne navigation equipment such as GPS due to the limitation of bridge, the visual servo method assumes that the camera can observe the bridge, so we only discuss the performance of contour detection algorithm when the USV is close to the bridge aperture. "Haixiang" collected a total of 65 images when it passed through the bridge aperture and we selected several typical images and analyzed them.

In Figure 11, the red frame is the contour of the bridge aperture given by the contour detection algorithm, and the green frame is the contour of the bridge aperture that was manually marked. The IOU of the intersection of the two on the horizontal axis represents the accuracy of the detection.

The IOU of the four figures below are 99.51%, 94.77%, 95.84% and 99.84% respectively. The average IOU of 65 images of bridge aperture crossing scenes is about 96%, which can meet the accuracy requirement of bridge aperture crossing algorithm by visual servo.

ISSN: 2414-1895 DOI: 10.6919/ICJE.202012_6(12).0041

(a) (b) (c) (d)

Figure 11. Contour detection of typical image

5. Conclusion

This paper presents a Visual servo-based method for bridge crossing of USV, which is used to accommodate outlier and loss of GPS signals near and under bridges so as to enhance the ability of USV to sail through the bridge safely. This method uses the brightness characteristics of the bridge aperture to simplify the extraction of bridge aperture contours in complex environments. Simulation and experiment results show that the proposed algorithm achieves 96% accuracy rate for bridge aperture detection, and 100% safe driving rate when the starting point is within a distance of 4m from the center line of the bridge, which basically meets the requirements for safe sailing of the USV through the bridge.

References

[1] Cao Juan,Wang Xuesong. Development status and future prospect of unmanned ships at home and abroad [J]. China Ship Survey,2018(05):94-97.[In chinese].

[2] Shi Jingli. Intelligent Ship " Mission at Sea " [J]. China Ship Survey,2019(11):32-43. [In chinese].

[3] Ko N Y, Choi H T, Lee C M, et al. [IEEE OCEANS 2016 MTS/IEEE Monterey -Monterey, CA, USA (2016.9.19-2016.9.23)] OCEANS 2016 MTS/IEEE Monterey -Navigation of unmanned surface vehicle and detection of GPS abnormality by fusing multiple sensor measurements[C]// Oceans. IEEE, 2016:1-5.

[4] Ko N Y, Jeong S, Choi H T, et al. Fusion of Multiple Sensor Measurements for Navigation of an Unmanned Marine Surface Vehicle[C]// International Conference on Control. IEEE, 2017.

[5] Woo J, Kim N. Vision based obstacle detection and collision risk estimation of an unmanned surface vehicle[C]// International Conference on Ubiquitous Robots & Ambient Intelligence. IEEE, 2016.

[6] Wang H, Wei Z, Ow C S, et al. Improvement in real-time obstacle detection system for USV[C]// International Conference on Control Automation Robotics & Vision. IEEE, 2013.

[7] Wang H, Wei Z. Stereovision based obstacle detection system for unmanned surface vehicle[C]// IEEE International Conference on Robotics & Biomimetics. IEEE, 2013.

[8] Almeida C , Franco T , Ferreira H , et al. [IEEE OCEANS 2009-EUROPE (OCEANS) - Bremen, Germany (2009.05.11-2009.05.14)] OCEANS 2009-EUROPE - Radar based collision detection developments on USV ROAZ II[J]. 2009:1-6.

[9] J. Muhovič, R. Mandeljc, B. Bovcon, M. Kristan and J. Perš, "Obstacle Tracking for Unmanned Surface Vessels Using 3-D Point Cloud," in IEEE Journal of Oceanic Engineering, vol. 45, no. 3, pp. 786-798, July 2020, doi: 10.1109/JOE.2019.2909507.

[10] Han J, Park J, Kim T, et al. Precision navigation and mapping under bridges with an unmanned surface vehicle[J]. Autonomous Robots, 2015, 38(4):349-362.

[11] JungwookH,Jinwhan K.Three-Dimensional Reconstruction of a Marine Floating Structure With an Unmanned Surface Vessel[J]. IEEE Journal of Oceanic Engineering, 2018, PP:1-13.

[12] Huang Yitian, Zhu Xiaohui, et al. Obstacle Detection and Map Construction of Unmanned Boat Based on StereoVision [J]. Computer Measurement & Control, 2019(8). [In chinese].

[13] Yang Zhao,Wang Jianhua,. Straight Line Path Following of Unmanned Surface Vessel Based on Fuzzy PID [J].Computer Engineering,2014,40(10):270-274+2.[In chinese].